Irreversibility in Heisenberg Spin Systems. III. Kinetic Equations for the Autocorrelation Function at Finite Temperature

P. RÉSIBOIS AND M. DE LEENER*
Université Libre, Brussels, Belgium
(Received 14 August 1968)

Recently the authors have derived kinetic equations describing the behavior of the spin autocorrelation function $\Gamma_q(t)$ in a Heisenberg system at infinite temperature. In the present paper, this derivation is extended to finite temperatures (above the critical point). It is shown that, in the Weiss limit where the number of neighbors $Z\to\infty$, the effects of the equilibrium (Ornstein-Zernicke) correlations present in the system at the initial time can be entirely incorporated within an effective temperature-dependent interaction which governs the temporal behavior of the autocorrelation function (af). A non-Markoffian kinetic equation is obtained in which the kernel is highly nonlinear in the *complete* af $\Gamma_q(t)$; this contrasts with the infinite-temperature case, where the kernel was a functional of the direct af only. This new feature leads to simple approximations near the critical point, as will be discussed in detail in the next paper of this series.

I. INTRODUCTION

IN two recent papers,[1,2] the authors have analyzed the spin autocorrelation functions (af)

$$\Gamma_{ab}{}^{\alpha\beta}(t)=\langle S_a{}^{\alpha}(t)S_b{}^{\beta}(0)\rangle \tag{1.1}$$

of a Heisenberg system of spins $s=\frac{1}{2}$ in the high-temperature limit. Here, $S_a{}^{\alpha}(t)$ denotes the Heisenberg representation of spin component $\alpha(\alpha=+,-,z)$ at lattice point a, and the bracket indicates the average over the equilibrium distribution.

Exact kinetic equations were obtained, in the limit of a large number of neighbors, by a systematic reorganization of the perturbation series for $\Gamma_{ab}{}^{\alpha\beta}(t)$. More precisely, it was shown that the direct af $\Gamma(t)$ $[\Gamma(t)\equiv 4\Gamma_{aa}{}^{zz}(t)]$ obeys the nonlinear equation

$$\partial_t\Gamma(t)=-\int_0^t \tilde{G}_0(t'|\Gamma)\Gamma(t-t')dt', \tag{1.2}$$

while the Fourier transform $\Gamma_q(t)$ of the af is given by

$$\partial_t\Gamma_q(t)=\int_0^t [\tilde{G}_q(t'|\Gamma)-\tilde{G}_0(t'|\Gamma)]\Gamma_q(t-t')dt', \tag{1.3}$$

which is linear once $\Gamma(t)$ has been determined from (1.2). In these equations, the non-Markoffian kernel $\tilde{G}_q(t|\Gamma)$ is a nonlinear functional of Γ and, as such, satisfies the condition

$$\tilde{G}_q(t|\Gamma)\to 0 \quad (t\to\infty). \tag{1.4}$$

Although this kernel is defined as an infinite series of terms, simple approximations have been proposed, which allow the kinetic equations (1.2) and (1.3) to be solved explicitly.

The main results thus obtained can be summarized as follows:

(1) $\Gamma(t)$ starts with a Gaussian behavior but finally approaches zero through damped oscillations. The origin of this behavior can be found in the non-Markoffian nature of Eq. (1.2), where the characteristic decay time of the kernel $\tilde{G}_0(t|\Gamma)$ is of the same order of magnitude as the decay time of the function $\Gamma(t)$ itself.

(2) In the small-wave-number limit $q\to 0$, Eq. (1.3) tends asymptotically to a Markoffian diffusion equation because we then have a complete separation between the characteristic time of $\Gamma(t)$ (and thus of $[\tilde{G}_q(t|\Gamma)-\tilde{G}_0(t|\Gamma)]$) and the very large decay time ($\sim q^{-2}$) of $\Gamma_q(t)$.

Although these results are interesting as such and can be applied to a variety of experimental situations,[3] there remains the very important question of generalizing them to finite temperature. In particular, we would like to discuss in a similar frame the behavior of (1.1) near the critical point, where traditional theories run into severe difficulties.[4] In this paper, we derive formal kinetic equations for the af valid at any temperature above the Curie point T_C. Approximate solutions of these equations for ferromagnets near T_C will be presented in the next paper of this series.

The method used has already been discussed in detail in RDL I. It is based on a formal solution of the Liouville-von Neumann equation as developed by Prigogine and co-workers in their study of nonequilibrium processes in quantum gases.[5] In Sec. II, we briefly recall the basic formulas of this approach; however, the equations there are mainly quoted for further use and the reader is urged to refer to RDL I (Sec. II mainly) for further explanations.

The main difference between the present calculation and the infinite-temperature case is the existence of equilibrium correlations which will, or course, influence the dynamical evolution of the system; in the Weiss

* Chargé de Recherches au Fonds National de la Recherche Scientifique de Belgique.

[1] P. Résibois and M. De Leener, Phys. Rev. **152**, 305 (1966) (hereafter referred to as RDL I).

[2] M. De Leener and P. Résibois, Phys. Rev. **152**, 318 (1966) (hereafter referred to as RDL II).

[3] See, for instance, P. Résibois, P. Borckmans, and D. Walgraef, Phys. Rev. Letters **17**, 1290 (1966).

[4] See W. Marshall, Natl. Bur. Std. (U. S.), Misc. Publ. **273**, 135 (1966).

[5] I. Prigogine, *Non Equilibrium Statistical Mechanics* (Interscience Publishers, Inc., New York, 1962); P. Résibois, Physica **27**, 541 (1961).

limit ($Z\to\infty$, where Z is the number of neighbors), they are described by the well-known Ornstein-Zernicke law and become of long range near T_C.[6] In Sec. III, we build the density matrix which describes our spin system at time $t=0$, taking these correlations into account.

Section IV is devoted to a generalization of the diagram technique introduced in RDL I. We represent by graphs the formal perturbation expansion of (1.1), including the equilibrium part.

Using this diagram technique, it is fairly easy to determine which contributions dominate in the Weiss limit; this is the object of Sec. V.

In Sec. VI, we analyze in detail the effect of the equilibrium Ornstein-Zernicke-type correlations on the dynamics of the system: Limiting ourselves to the Weiss limit, we show that they can be entirely incorporated in a so-called "vertex renormalization" which replaces the exchange coupling between the spins by an effective temperature-dependent interaction.

With this result, we are then left with a purely dynamical problem, which presents the same difficulty as its infinite-temperature limit. Namely, straightforward perturbation calculus is not possible because the lowest-order transition probability between two given spins grows like t^2 instead of t as in the usual scattering problems. A key to this problem is given which parallels closely the infinite-temperature case discussed in RDL I. It is suggested that one is not allowed to consider a given finite number of spins as isolated, since they are imbedded in the rest of the system, i.e., in a "bath" which dissipates the magnetization put on these given spins. We develop in Sec. VII a renormalization scheme that expresses this idea; however, this scheme is slightly more general than in the infinite-temperature problem. There, indeed, the renormalization was done with the help of the *direct* af $\Gamma(t)$ [see (1.1), (1.2), and (1.3)], which essentially describes the *short-distance* behavior of the system. Although formally correct, this procedure is not adequate in general since, near the critical point, we expect long-range effects (in both space and time) to be essential; it thus appears natural to renormalize the graphs in terms of the complete af

$$\tilde{\Gamma}_q(t)=\Gamma_q(t)/\Gamma_q(0).$$

Once this program is achieved, it is fairly easy to derive a kinetic equation for $\tilde{\Gamma}_q(t)$. We show in Sec. VIII that $\tilde{\Gamma}_q(t)$ obeys a nonlinear non-Markoffian equation of the following form:

$$\partial_t\tilde{\Gamma}_q(t)=\int_0^t \tilde{G}_q(t-t'|\tilde{\Gamma}_{q'})\tilde{\Gamma}_q(t')dt', \tag{1.5}$$

where the kernel $\tilde{G}_q$ is now a nonlinear functional of $\tilde{\Gamma}_{q'}$ (for all q') itself. Rules are given which allow to compute this kernel as an infinite series of terms, each obeying a property analogous to (1.4); note that this kernel is, of course, temperature-dependent, a fact which has not been explicitly exhibited in the notation used in (1.5).

A few formal proofs have been relegated to appendices; moreover, we have not detailed any explicit calculation obviously analogous to a similar development given in the infinite-temperature case.

II. FORMAL PRELIMINARIES

We have shown[7] in RDL I that the af (1.1) can be written as

$$\Gamma_{ab}{}^{\alpha\beta}(t)=\mathrm{Trace}[S_a{}^{\alpha}\rho^{\beta}(t|b)], \tag{2.1}$$

where the operator $\rho^{\beta}(t|b)$ is the solution of the von Neumann equation

$$i\partial_t\rho^{\beta}(t|b)=\lambda[H,\rho^{\beta}(t|b)], \tag{2.2}$$

subject to the initial condition

$$\rho^{\beta}(0|b)=S_b{}^{\beta}\rho^{eq}, \tag{2.3}$$

ρ^{eq} being the canonical distribution ($\beta=1/kT$):

$$\rho^{eq}=\exp[-\beta H]/\mathrm{Trace}[\exp-\beta H]. \tag{2.4}$$

Note that in Eq. (2.2) we have introduced a counting parameter λ, which we shall set equal to one at the end of the calculation (see Ref. 10).

In order to solve (1.2), we introduce the following representation for the matrix elements of any operator A in the localized spin representation

$$|m\rangle=\prod_{i=1}^{n}|m_i\rangle\,(m_i=\pm\tfrac{1}{2})$$

$$\langle m|A|m'\rangle=A_{\mu}(M), \tag{2.5}$$

with

$$\mu=m-m',\quad M=\tfrac{1}{2}(m+m'). \tag{2.6}$$

Here, as well as in all further formal expressions, we use the compact notation $m=\{m_1,m_2,\cdots,m_N\}$, $\mu=\{\mu_1,\mu_2,\cdots,\mu_N\}$, etc. In this representation, the formal solution of Eq. (2.2) leads to the following expansion for the matrix elements $\rho_{\mu}{}^{\beta}(M;t|b)$ of the operator $\rho^{\beta}(t|b)$ [see RDL I (II.21)]:

$$\rho_{\mu}{}^{\beta}(M;t|b)=\sum_{n=0}^{\infty}\left(\frac{\lambda}{i}\right)^n\int d\tau^n\sum_{\mu'}\langle\mu|[\mathfrak{IC}(M)]^n|\mu'\rangle \times\rho_{\mu'}{}^{\beta}(M;0|b), \tag{2.7}$$

where the "Liouville-von Neumann operator" is defined by

$$\langle\mu|\mathfrak{IC}(M)|\mu'\rangle=\eta^{\mu'}H_{\mu-\mu'}(M)\eta^{-\mu}-\eta^{-\mu'}H_{\mu-\mu'}(M)\eta^{\mu}. \tag{2.8}$$

[6] R. Brout, *Phase Transitions* (W. A. Benjamin, Inc., New York, 1965).

[7] Except when explicitly mentioned, we follow the notation of RDL I and II.

In this expression, we used the displacement operator $\eta^{\pm\mu}$, which acts on an arbitrary function of M in the following way:

$$\eta^{\pm\mu}f(M)=f(M\pm\tfrac{1}{2}\mu). \tag{2.9}$$

The decomposition of the Heisenberg Hamiltonian in transverse and longitudinal pair interactions, induces a similar separation of the operator $\mathcal{H}$:

$$\langle\mu|\mathcal{H}(M)|\mu'\rangle=\sum_{i\neq j}[\langle\mu|\mathcal{H}_{ij}{}^{+-}|\mu'\rangle+\langle\mu|\mathcal{H}_{ij}{}^{zz}|\mu'\rangle] \tag{2.10}$$

and the two-body operators $\mathcal{H}_{ij}{}^{+-}$ and $\mathcal{H}_{ij}{}^{zz}$ obey fairly simple selection rules; their explicit form, already established in RDL I (II.16) to (II.19) is reproduced in Appendix A.

In RDL I, we also established the following results:

$$\Gamma_{ab}{}^{zz}(t)=\rho^{z}(M_a=\tfrac{1}{2};t|ab) \tag{2.11}$$

and

$$\Gamma_{ab}{}^{+-}(t)=\rho^{-}(M_a=0;t|ab), \tag{2.12}$$

where the *reduced* density matrices appearing on the right-hand side are partial traces of the matrix elements given by (2.7):

$$\rho^{z}(M_a;t|ab)=\sum_{\{M_{i\neq a}\}}\rho_0{}^{z}(M;t|b) \tag{2.13}$$

and

$$\rho^{-}(M_a;t|ab)=\sum_{\{M_{i\neq a}\}}\rho_{-1_a}{}^{-}(M;t|ab). \tag{2.14}$$

Note that the information given by (2.11) and (2.12) is redundant, since the rotational invariance of (1.1) implies that

$$\Gamma_{ab}{}^{+-}(t)=2\Gamma_{ab}{}^{zz}(t)=\tfrac{1}{2}\Gamma_{ab}(t), \tag{2.15}$$

the last equality defining the function $\Gamma_{ab}(t)$.

We shall also be interested in the Fourier transform of these functions, for instance,

$$\Gamma_q(t)=\sum_a \exp[iq(a-b)]\Gamma_{ab}(t). \tag{2.16}$$

Since it is known that the equilibrium correlation function $\Gamma_q(0)$ has a singular behavior for $q\to 0$ at the critical point, it is useful to separate this singularity by defining a normalized af

$$\tilde{\Gamma}_q(t)=\Gamma_q(t)/\Gamma_q(0), \tag{2.17}$$

such that $\tilde{\Gamma}_q(0)=1$. Similar definitions hold for $\tilde{\Gamma}_q{}^{zz}(t)$ and $\tilde{\Gamma}_q{}^{+-}(t)$. In configurational space, Eq. (2.17) is equivalent to

$$\Gamma_{ab}(t)=\sum_s \tilde{\Gamma}_{as}(t)\Gamma_{sb}(0). \tag{2.18}$$

III. INITIAL CONDITION AND EQUILIBRIUM DENSITY MATRIX

Let us write the initial condition (2.3) in the $\mu-M$ variables. We have, from (2.3),

$$\rho_\mu{}^{\beta}(M;0|b)=\langle M+\tfrac{1}{2}\mu|S_b{}^{\beta}\rho^{eq}|M-\tfrac{1}{2}\mu\rangle, \tag{3.1}$$

which becomes, in the particular case $\beta=z$,

$$\begin{aligned}\rho_\mu{}^{z}(M;0|b)&=(M_b+\tfrac{1}{2}\mu_b)\langle M+\tfrac{1}{2}\mu|\rho^{eq}|M-\tfrac{1}{2}\mu\rangle\\&=(M_b+\tfrac{1}{2}\mu_b)\rho_\mu{}^{eq}(M).\end{aligned} \tag{3.2}$$

Since $M_b=0$ when $\mu_b=\pm 1$, while $\mu_b=0$ when $M_b\neq 0$ [see (2.6)], this result can still be rewritten as

$$\rho_\mu{}^{z}(M;0|b)=(M_b\delta_{\mu_b,0}{}^{\mathrm{Kr}}+\tfrac{1}{2}\mu_b\times\delta_{\mu_b,0}{}^{\mathrm{Kr}})\rho_\mu{}^{eq}(M). \tag{3.3}$$

Similar formulas hold for $\rho_\mu{}^{\pm}(M;0|b)$, which will, however, not be needed here.

From (3.3), it is obvious that the only problem in the calculation of the initial state $\rho_\mu{}^{\beta}(M;0|b)$ is the explicit evaluation of the canonical density matrix ρ^{eq}. In principle, we should start from the general expansion

$$\rho^{eq}=\sum_{n=0}^{\infty}\frac{\beta^n}{n!}(-H)^n\Big/\mathrm{Trace}\Big[\sum_{n=0}^{\infty}\frac{\beta^n}{n!}(-H)^n\Big]. \tag{3.4}$$

We should then generalize to our time-dependent problem the techniques developed for the equilibrium situation and establish a linked cluster expansion for the spin af. Then, limiting ourselves to the Weiss approximation $Z\to\infty$, we should look for the leading terms in an expansion in powers of Z^{-1}. These tedious though simple manipulations have been accomplished in detail but, in order to avoid superfluous lengthiness, we shall use a short-cut, the validity of which should become evident once it is noticed that the dimensionless parameters appearing in the expansions of the dynamical ($\sim t$) and of the equilibrium ($\sim\beta$) parts are different. From what is known in the equilibrium theory (see Ref. 6), we may infer that, *in the Weiss limit and for $T>T_C$, the dominant terms in the equilibrium density matrix correspond to pair correlations, described by the Ornstein-Zernicke law, both for the diagonal and for the off-diagonal matrix elements.*

Under these conditions, we thus write

$$\begin{aligned}\rho_\mu{}^{eq}(M)=\frac{1}{2^N}\sum_{\substack{(ij)\\(st)}}\prod_{(ij)}\{\varphi_n(M_i,M_j)[&\delta_{\mu_i,1}{}^{\mathrm{Kr}}\delta_{\mu_j,-1}{}^{\mathrm{Kr}}\\&+\delta_{\mu_i,-1}{}^{\mathrm{Kr}}\delta_{\mu_j,+1}{}^{\mathrm{Kr}}]\}\prod_{(st)}\{\varphi_d(M_s,M_t)\\&\times\delta_{\mu_s,0}{}^{\mathrm{Kr}}\delta_{\mu_t,0}{}^{\mathrm{Kr}}\}\prod_{\alpha}\delta_{\mu_\alpha,0}{}^{\mathrm{Kr}},\end{aligned} \tag{3.5}$$

where the sum runs over all possible distinct ways of dividing the system into n_1 pairs of spins (ij), n_2 pairs of spins (st) and $N-2(n_1+n_2)$ remaining spins α. The functions φ_n and φ_d, respectively, describe the transverse and longitudinal pair correlations in the Weiss approximation:

$$\begin{aligned}\varphi_n(M_i,M_j)&=\beta\Phi_{ij}\delta_{M_i,0}{}^{\mathrm{Kr}}\delta_{M_j,0}{}^{\mathrm{Kr}},\\\varphi_d(M_i,M_j)&=2\beta\Phi_{ij}M_iM_j,\end{aligned} \tag{3.6}$$

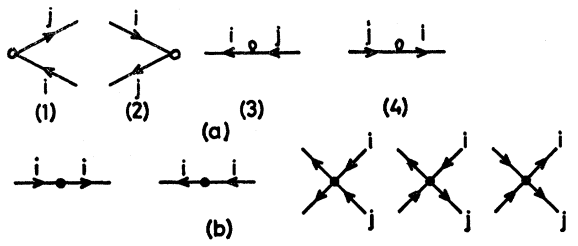

FIG. 1. The elementary dynamical vertices: (a) transverse; (b) longitudinal.

where

$$\Phi_{ij}=\frac{1}{N}\sum_q \phi_q \exp[iq(i-j)], \tag{3.7}$$

$$\phi_q=J_q/(1-\tfrac{1}{2}\beta J_q), \tag{3.8}$$

and J_q denotes the Fourier transform of the exchange interaction.

Let us stress once more that Eq. (3.5) can be proved in the Weiss limit. Its physical content is, however, self-evident; moreover, the function Φ_{ij} appearing in (3.6) and (3.7) is well known from equilibrium theory, while the M-dependent factors in these equations are easily verified by computing the matrix elements of (3.4) to first order in β, in the $\mu-M$ variables.

From (3.5), one can easily check that the equilibrium correlation functions have the usual Weiss form [see (2.1, 2.3 and 2.15)]:

$$\Gamma_{ab}(0)=4\Gamma_{ab}{}^{zz}(0)=2\Gamma_{ab}{}^{+-}(0)$$
$$=\delta_{a,b}{}^{\mathrm{Kr}}+(1-\delta_{a,b}{}^{\mathrm{Kr}})\tfrac{1}{2}\beta\Phi_{ab}. \tag{3.9}$$

IV. DIAGRAM TECHNIQUE

Equations (2.7), (3.3), and (3.5) furnish a well-defined expansion for the evaluation of the spin af. To analyze this expression, it is very useful to generalize the diagrammatic representation introduced in RDL I.

We first draw a vertical line which corresponds to $t=0$. On the left of this line, we then represent the various contributions to the dynamical expansion (2.7) as in the infinite temperature case. In this expansion, starting from the initial state $|\mu'\rangle$, the sequence of operators describes a series of transitions which bring the system through the states $|\mu'\rangle\to|\mu''\rangle\to\cdots$ to the final state $|\mu\rangle$. Each of these states is represented by horizontal arrowed lines corresponding to the various $\mu_j\neq 0$, a plain line j with an arrow pointing to the left (or right) describing a state with $\mu_j=+1$ (or -1). Each interaction $\mathcal{H}(M)$ then introduces a transition represented by a vertex, either transverse or longitudinal. Transverse vertices involve a loop while longitudinal vertices involve a dot; these vertices are shown in Fig. 1 and their analytical contributions,

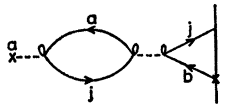

FIG. 2. A typical dynamical graph of order 3 ($\{\mu'\}=1_b,-1_j,\{0\}'$).

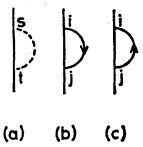

FIG. 3. Diagrammatic representation of the equilibrium correlations: (a) longitudinal; (b) and (c) transverse.

already established in RDL I, are recalled in Appendix A. In addition to the arrowed lines, we also introduce semiconnection (dotted) lines, which appear whenever a spin i is in a state $\mu_i=0$, between two vertices where it interacts. Finally, both specified spins b and a [see (1.1)] are represented by a cross, drawn respectively on the vertical line (at $t=0$) and at the left end of the graph (at time t); whenever spin b (or a) starts (or ends) in a diagonal state $\mu_b=0$ (or $\mu_a=0$), we link the corresponding cross to its first (or last) interaction in the dynamical part by a semiconnection line. An example of the dynamical part of a diagram is given in Fig. 2.

Of course, we also need a diagrammatic representation of the particular initial state (3.3) and (3.5) which appears in a given contribution. This will be drawn on the *right* of the vertical line and, because (3.5) only involves independent pair correlations, the graphs will be fairly simple. For each longitudinal correlation $\varphi_a(M_s,M_t)$ we draw a loop with spin indices s and t at its ends [see Fig. 3(a)]. Similarly, an arrowed plain loop with two spin indices i and j represents a transverse correlation $\varphi_n(M_i,M_j)$. Note that the two cases where the arrow points either from j to i or from i to j must be considered distinctly, since they correspond to the two terms of (3.5) where, respectively, $\mu_i=-1$, $\mu_j=+1$, and $\mu_i=+1$, $\mu_j=-1$ (see Fig. 3b). Uncorrelated spins are not represented.

In order to build the complete graphs, with both dynamical and equilibrium parts, we match together the lines (and their spin indices) appearing on the right and on the left of the vertical line; we have, however, to extend slightly the notion of semiconnection bond. If a spin is in a state of longitudinal correlation ($\mu_i=0$) at $t=0$ and has some dynamical interaction at time t' ($t'>0$), we draw a semiconnection line for this spin between 0 and t'. Examples are given in Fig. 4.

At this stage, we should prescribe the rules giving the contribution associated to a given graph. We shall, however, postpone the formulation of these rules and first establish the following theorem which considerably reduces the number of graphs to be considered.

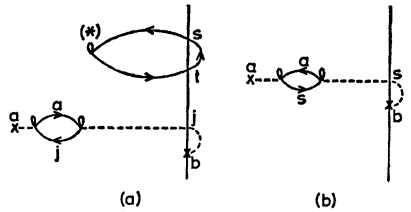

FIG. 4. Two contributions to $\rho_0{}^s(M_a;t|b)$.

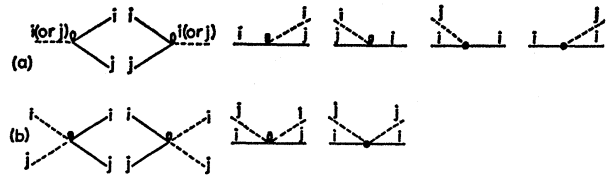

FIG. 5. Elementary vertices with semiconnection bonds: (a) one semiconnection bond; (b) two semiconnection bonds.

Theorem I: For $T>T_C$, the only nonvanishing contributions correspond to graphs built with vertices involving at least one semiconnection line. Similarly, any spin different from b appearing in a longitudinal equilibrium correlation must be semiconnected to the dynamical part of the graph.

The proof of this theorem is based on the observation that we are interested in the reduced density matrix (2.13) and (2.14) and thus have to take a trace over all spin variables $\{M_{i\neq a}\}$. The first part of the theorem is then exactly analogous to the Theorems I and II established in RDL I. The second part is based on the remark that if spin j appears in a longitudinal correlation, we obtain from (3.7) a factor

$$\varphi_d(M_i,M_j)=2\beta\Phi_{ij}M_iM_j. \tag{4.1}$$

If j does *not* appear in the dynamical part (as is implied by the absence of semiconnection), we may shift the trace over M_j in front of (4.1), and we get

$$\sum_{M_j}\varphi_d(M_i,M_j)=2\beta\Phi_{ij}M_i\sum_{M_j=\pm1}M_j=0. \tag{4.2}$$

This, of course, does not occur if $j\equiv b$, because in this case we have an additional M_b factor coming from (3.3). As an illustration of this theorem, the graph of Fig. 4(a) gives zero, because the starred vertex involves no semiconnection line.

Because each vertex has to be at least once semiconnected, it is convenient to consider the semiconnection bonds as integrant parts of the vertices. We have then the elementary vertices represented in Fig. 5, where the arrows have not been indicated. Note that the vertices corresponding to the last three graphs of Fig. 1(b) have no counterpart in Fig. 5. From Theorem I, the contribution of graphs involving these vertices identically vanish.

Although we shall later find stronger restrictions on the type of graphs when going explicitly to the Weiss limit $Z\to\infty$ (which until now has only been taken in the equilibrium part), let us now state the rules for calculating $\rho^z(M_a;t|ab)$ [and hence $\Gamma_{ab}{}^{zz}(t)$ from Eq. (2.11)].[8]

Rules A: (1) Draw all possible graphs ending at time t with a crossed dotted line a, consistent with the initial condition (3.3) and (3.5) and with the vertices of Fig. 5. Each equilibrium correlation must be connected or semiconnected to the dynamical part (except for spin b).[9]

(2) For each graph, associate a factor $2\beta M_sM_t\Phi_{st}$ to each longitudinal correlation (st) and a factor $\beta\delta_{M_i,0}{}^{\mathrm{Kr}}\delta_{M_j,0}{}^{\mathrm{Kr}}\Phi_{ij}$ to each transverse correlation (ij) [see (3.6)].

(3) Associate a factor $\delta_{M_i,0}{}^{\mathrm{Kr}}$ to each plain line (see the remark in Appendix A).

(4) Associate a factor M_b if the cross at time $t=0$ is on the dotted line b, or a factor $\frac{1}{2}\mu_b$ if it is on a plain line with index μ_b [see (3.3)].

(5) Associate a factor $(-J_{ij})\eta_{ij}$ to each transverse vertex and a factor $(-2J_{ij})(\mu_iM_j+\mu_jM_i)$ to each longitudinal vertex. The operator η_{ij} introduced in Appendix A is defined as

$$\eta_{ij}=\eta^{-1_i}\eta^{+1_j}-\eta^{+1_i}\eta^{-1_j}. \tag{4.3}$$

Operators and M-dependent factors should be ordered as they appear in the graph.

(6) Multiply by $(\frac{1}{2})^m(\lambda/i)^n\int d\tau^n$ for a graph of order n involving m spins, including a and b.

(7) Take the trace $(\sum_{M_i=\pm1}\cdots)$ over all spins appearing in the graph and different from a.

(8) Sum over all dummy spin indices.

From these rules, one easily verifies that the contribution associated with Fig. 4(b) is

$$(\tfrac{1}{2})^3\sum_s\sum_{M_s,M_b}\left(\frac{\lambda}{i}\right)^2\int d\tau^2(-J_{as})^2[\eta_{sa}\delta_{M_s,0}{}^{\mathrm{Kr}}\delta_{M_a,0}{}^{\mathrm{Kr}}\eta_{as}]\times2M_sM_b{}^2\beta\Phi_{sb}. \tag{4.4}$$

V. WEISS LIMIT

The diagram technique developed in Sec. IV is of little practical use for an arbitrary number of neighbors. Moreover, it should be kept in mind that the equilibrium correlations have already been expressed in a form which is only correct in the Weiss limit $Z\to\infty$. In this section, we establish the order of magnitude of an arbitrary graph in this same limit and extract therefrom the dominant contributions.

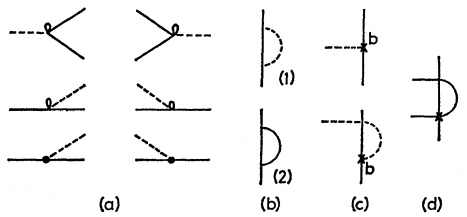

FIG. 6. Basic components of the dominant graphs in the Weiss limit: (a) elementary vertices; (b) equilibrium correlations; (c) nonequilibrium initial states for $\mathrm{Re}\Gamma_{ab}{}^{zz}$; (d) nonequilibrium initial state for $\mathrm{Im}\Gamma_{ab}{}^{zz}$ (arrows are not indicated).

[8] To make tedious things as short as possible, we limit ourselves to the zz component of the af. There is no difficulty in extending the present rules to the transverse component.

[9] For longitudinal correlations, this is a consequence of Theorem I; for transverse correlations, this condition has to be satisfied because we need at least one transition to bring the system from the nondiagonal initial state $\{\mu_i\neq0\}$ to the final diagonal state $\{\mu_i=0\}$.

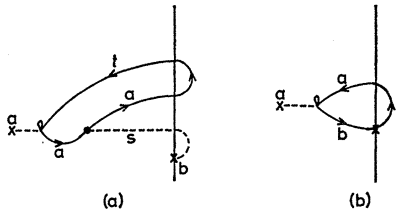

FIG. 7. Simple examples of dominant graphs: (a) for $\mathrm{Re}\Gamma_{ab}{}^{zz}(t)$; (b) for $\mathrm{Im}\Gamma_{ab}{}^{zz}(t)$.

In principle, our problem involves five parameters, t, Z, β, J and the lattice distance d. This latter quantity is, however, of no use in the present discussion. Moreover, Z, β, and J cannot be considered as independent. Indeed, for temperatures close to the critical point T_C, we have (see, for instance, Ref. 6):

$$\beta ZJ \simeq 1 , \tag{5.1}$$

whence it is easily shown that

$$\beta\Phi_{ij} \sim O(1/Z) \quad (i \neq j). \tag{5.2}$$

Since, in our problem, β only enters in the combination $\beta\Phi_{ij}$, we may disregard this parameter completely and estimate it with the help of (5.2). Thus, although the function Φ_{ij} is itself a complicated expression in J [see (3.7) and (3.8)], we may limit ourselves in analyzing the J dependence of the dynamical part only. In this part, J has been scaled by the parameter λ and we are thus left with the problem of analyzing the (λ, Z, t) dependence of the graph.[10]

When the temperature is far above T_C, (5.1) is, of course, replaced by

$$\beta ZJ = \alpha \ll 1 , \tag{5.3}$$

and we should, in principle, introduce this new smallness parameter. We shall, however, limit ourselves in estimating the graphs in regime (5.1) since this temperature region is by far the most interesting one. Moreover, our results can be easily applied to the situation (5.3) by expanding them in powers of α.

In the Weiss limit $Z \to \infty$, the following theorem holds.

Theorem II: (a) *Among the even terms in* λ, *which are all purely real, the dominant graphs are of order* $\lambda^2 \times (\lambda^2 Z)^{n-1} t^{2n}$ *for the indirect af* $(a \neq b)$ *and of order* $(\lambda^2 Z)^n t^{2n}$ *for the direct af.*

(b) *Among the odd terms in* λ, *which are all purely imaginary, the dominant graphs are of order* $\lambda^2(\lambda^2 Z)^{n-1} \times t^{2n+1}$ *for the indirect af and of order* $\lambda(\lambda^2 Z)^n t^{2n+1}$ *for the direct af.*

The proof is a generalization of that given in RDL I for $\beta = 0$. It has been relegated in Appendix B, where we also show that Theorem II furnishes precise information about the structure of the dominant graphs. To formulate this information, it is useful to extend slightly our nomenclature by introducing the concept of a *nonequilibrium initial state.* In the initial condition (3.3), spin b plays a special role because it is the only one which has been taken out of equilibrium. Two cases may occur:

(a) Spin b is not involved in any correlation at $t=0$ [Fig. 6(c)(1)].

(b) Spin b is involved in a transverse [Fig. 6(d)] or a longitudinal [Fig. 6(c)(2)] correlation; these we call nonequilibrium initial correlations. These three possible pieces of graphs describe the nonequilibrium initial state of the system. On the contrary, all the remaining correlations, which involve pairs of spins both different from b, correspond to equilibrium correlations [Fig. 6(b)(1) and 6(b)(2)].

With these definitions, it is shown in Appendix 3 that the real part of $\Gamma_{ab}{}^{zz}(t)$ [see, also, (2.11)], which behaves like

$$\mathrm{Re}\Gamma_{ab}{}^{zz}(t) = \sum_{n=0}^{\infty} \alpha_n \frac{1}{Z} (\lambda^2 Z t^2)^n \quad (a \neq b), \tag{5.4}$$

is the sum of all graphs built only with the elementary vertices of Fig. 6(a), the equilibrium correlations of Fig. 6(b) and the nonequilibrium initial states of Fig. 6(c). An example is given in Fig. 7(a). On the contrary, the imaginary part of $\Gamma_{ab}{}^{zz}(t)$ behaves like

$$\mathrm{Im}\Gamma_{ab}{}^{zz}(t) = \sum_{n=0}^{\infty} \beta_n \frac{\lambda t}{Z} (\lambda^2 Z t^2)^n \quad (a \neq b) \tag{5.5}$$

and is constructed with the elements of Fig. 6 [(a), (b), and (d)]; an example is shown in Fig. 7(b).

From (5.4) and (5.5), it is apparent that the time behavior of the af will be governed by the characteristic time

$$\tau_d \sim (Z^{1/2}\lambda)^{-1}. \tag{5.6}$$

Thus, we shall be interested in the formal expansions (5.4) and (5.5) for times t of the order of (5.6). Since, from (5.1), the Weiss limit implies the double limiting procedure $Z \to \infty$ and $\lambda \to 0$, with $(\lambda Z) \sim kT_C$ finite, we have to take the limit $t \to \infty$ such that

$$\tau = t/\tau_d = (\lambda\sqrt{Z})t = t/\sqrt{Z} \tag{5.7}$$

remains *finite.* Under these conditions, (5.4) and (5.5) become

$$\mathrm{Re}\Gamma_{ab}{}^{zz}(t) \sim \frac{1}{Z} \sum_{n=0}^{\infty} \alpha_n \tau^{2n}, \tag{5.8}$$

$$\mathrm{Im}\Gamma_{ab}{}^{zz}(t) \sim \frac{1}{Z^{3/2}} \sum_{n=0}^{\infty} \beta_n \tau^{2n+1}. \tag{5.9}$$

This result indicates that in all cases where the real part of $\Gamma_{ab}{}^{zz}$ contributes to a physical property, we are

[10] This analysis motivates the introduction of a formal counting parameter λ in the von Neumann equation (2.2). With this trick, the order in λ gives the order in J for the dynamical part only.

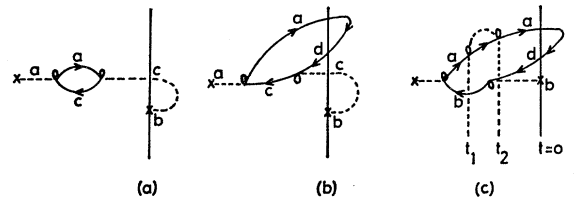

FIG. 8. Example of effective interaction: (a) purely dynamical graph; (b) effect of equilibrium correlations; (c) *non*-freely propagating equilibrium correlations.

allowed to neglect completely the imaginary part. In this paper, we limit our discussion to this situation and, except when otherwise stated, we shall henceforth use the notation

$$\Gamma_{ab}{}^{zz}(t) \equiv \mathrm{Re}\Gamma_{ab}{}^{zz}(t). \tag{5.10}$$

However, in the next paper of this series, we shall compare our theory with previous work on the subject and, to this aim, we shall also consider $\mathrm{Im}\Gamma_{ab}{}^{zz}(t)$, which can be calculated along the same lines; note that these imaginary and real parts are not independent quantities since they are related through the exact fluctuation-dissipation theorem.

VI. VERTEX RENORMALIZATION

For the sake of the discussion, let us consider the simple graph of Fig. 8(a). According to Rules A, its contribution to $\Gamma_{ab}{}^{zz}(t)$ is

$$\Gamma_{ab}{}^{zz}(t)\,|_{(8a)} = \left(\frac{\lambda}{i}\right)^2 \frac{t^2}{2!} \sum_c \sum_{M_c,M_b} [(-J_{ac})^2 \eta_{ac} \delta_{M_a,0}{}^{\mathrm{Kr}} \times \delta_{M_c,0}{}^{\mathrm{Kr}} \eta_{ca}] 2\beta\Phi_{cb} M_c M_b{}^2 (\tfrac{1}{2})^3 |_{M_a=1/2}. \tag{6.1}$$

Two difficulties of different natures are apparent in this expression:

(1) Precisely as in the infinite temperature case, the Born approximation (6.1) gives a transition probability which grows like t^2 instead of the t dependence of usual scattering problems. The solution to this problem will be obtained in Sec. VII by an adequate reorganization of the perturbation scheme.

(2) Another weakness of Eq. (6.1) is that, except for the nonequilibrium initial state, which involves $\beta\Phi_{cb}(\beta)$, no temperature dependence appears. In particular, the dynamical operator, which has been put between brackets in (6.1) has exactly the same form as for $\beta=0$. However, we expect physically that the equilibrium correlations present at $t=0$ should affect the dynamical evolution of the system.

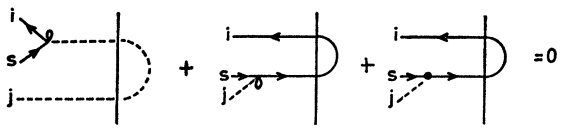

FIG. 9. Graphical formulation of Theorem III.

We shall now show that it is indeed possible to find such an effect by absorbing all equilibrium correlations in the definition of effective temperature-dependent interactions; in this way the new initial condition will involve, at most, the nonequilibrium correlation involving spin b. To illustrate this on a simple example, let us evaluate the contribution of Fig. 8(b). From Rules A, we get

$$\Gamma_{ab}{}^{zz}(t)\,|_{(8b)} = \left(\frac{\lambda}{i}\right)^2 \frac{t^2}{2!} \sum_{c,d} \sum_{M_c,M_d,M_b} [(-J_{ac})\eta_{ac}\delta_{M_a,0}{}^{\mathrm{Kr}} \times \delta_{M_c,0}{}^{\mathrm{Kr}} \eta_{cd}(-J_{cd})] \delta_{M_d,0}{}^{\mathrm{Kr}} \beta\Phi_{da} \times 2\beta\Phi_{cb} M_c M_b{}^2 (\tfrac{1}{2})^4 |_{M_a=1/2}. \tag{6.2}$$

The displacement operations and summation on M_d can be explicitly performed, with the result

$$\Gamma_{ab}{}^{zz}(t)\,|_{(8b)} = \left(\frac{\lambda}{i}\right)^2 \frac{t^2}{2!} \sum_c \sum_{M_b,M_c} (-J_{ac})\eta_{ac}\delta_{M_a,0}{}^{\mathrm{Kr}} \delta_{M_c,0}{}^{\mathrm{Kr}} \eta_c \times [\sum_d (-J_{cd}) \tfrac{1}{2}\beta\Phi_{da}] 2\beta\Phi_{cb} M_c M_b{}^2 (\tfrac{1}{2})^3 |_{M_a=1/2}, \tag{6.3}$$

where the displacement operator η_c is defined as

$$\eta_c = \eta^{-1_c} - \eta^{+1_c}. \tag{6.4}$$

If we use the following identity, easily established from (3.7) and (3.8),

$$\Phi_{ca} = J_{ca} + \sum_d J_{cd} \tfrac{1}{2}\beta\Phi_{da}, \tag{6.5}$$

and if we notice that, in (6.1), the operator η_{ca} may be replaced by η_c (because there is no M_a-dependent factor on the right), we can combine Eqs. (6.1) and (6.3) and find

$$\Gamma_{ab}{}^{zz}\,|_{(8a+8b)} = \left(\frac{\lambda}{i}\right)^2 \frac{t^2}{2!} \sum_c \sum_{M_b,M_c} [(-J_{ac})(-\Phi_{ac})\eta_{ac}\delta_{M_a,0}{}^{\mathrm{Kr}} \times \delta_{M_c,0}{}^{\mathrm{Kr}} \eta_c] 2\beta\Phi_{cb} M_c M_b{}^2 (\tfrac{1}{2})^3 |_{M_a=1/2}. \tag{6.6}$$

As announced, the effect of the equilibrium correlation has been included in the effective interaction $\Phi_{ac}(\beta)$, replacing in (6.6) one of the exchange interaction J_{ac} of (6.1).

The generalization of this result is, of course, very desirable. But it is clear that the reorganization that we have accomplished on the graph of Fig. 8(b) was possible only because of its particularly simple topology. Indeed, reading this graph in the direction of increasing times (from right to left), we see that the correlated spins a and d "propagate freely," i.e., do not participate in any interaction between the initial time $t=0$ and the time t_1 at which spin d is connected to the nonequilibrium initial state. This is essential in the derivation of (6.6).

Figure 8(c) shows a simple example where this is not the case; here the equilibrium correlation a-d is modified by a dynamical interaction at a time t_2 before t_1. In this case, the equilibrium correlation cannot be absorbed immediately in an effective interaction, as was done for Fig. 8(b). Fortunately, this difficulty is only apparent because all unpleasant graphs of this type combine to give zero! In other words, the following theorem holds:

Theorem III (of propagation of equilibrium): In the Weiss limit, the af $\Gamma_{ab}{}^{zz}(t)$ *is given by the sum of the contributions associated with the only graphs where all equilibrium correlations propagate freely until the time at which they connect to the nonequilibrium initial state.*

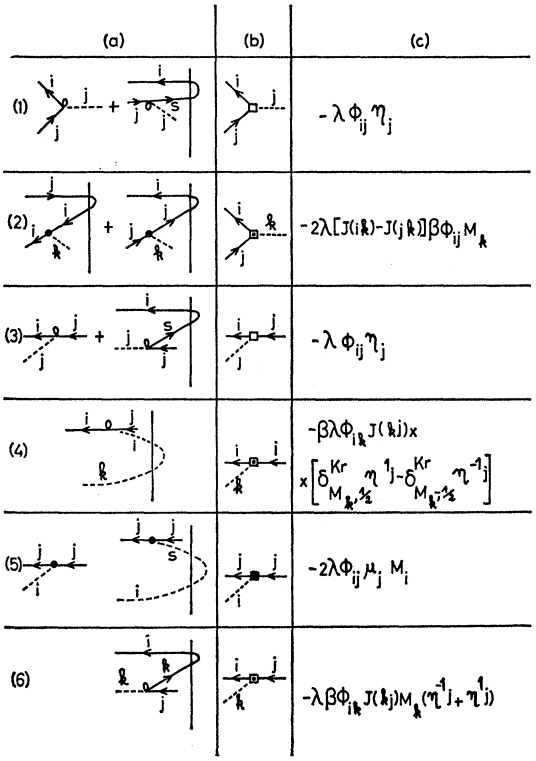

FIG. 10. Effective temperature-dependent vertices: (a) graphs to be combined; (b) effective vertices; (c) analytical contributions. The effective vertices (4) and (6) are drawn in the same way, because they always appear together; their contributions must then be added.

The physical content of this theorem is clear: In the Weiss limit, the Heisenberg Hamiltonian propagates the equilibrium Ornstein-Zernicke correlations. The formal proof of this result is very simple, but tedious. Let us consider, for example, a graph involving a longitudinal correlation between spins i and j and where the first dynamical interaction leads to the new state $\mu_i=+1$, $\mu_s=-1$, $\mu_j=0$. As shown in Fig. 9, we can combine this graph with two other contributions leading to the same state $\mu_i=+1$, $\mu_s=-1$, $\mu_j=0$ after one dynamical interaction. Using Rules A, it can be verified explicitly

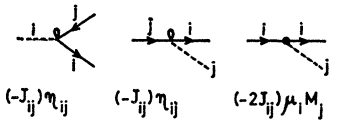

FIG. 11. Nonrenormalizable vertices: the analytical contribution of each vertex is given just below.

that the sum of these three graphs vanishes. The other cases are treated similarly.

We can now generalize the result of Eq. (6.6), i.e., incorporate any freely propagating equilibrium correlation in an effective temperature-dependent dynamical vertex at time t_1, where t_1 is the time at which this equilibrium correlation connects to the nonequilibrium initial state of the graph.[11] In Fig. 10,[12] we have indicated how the various effective vertices are defined. The first column gives the graphical structures which are combined to give the different effective temperature-dependent interactions; these are represented by the new square vertices in the second column. The third column gives the analytical contribution associated to them.

The calculations leading to these results run as in the example of Fig. 8(a) and (b) and will not be reproduced here. Let us just notice that in certain cases, the effective vertex involves *three* different spins; this case offers, however, no particular difficulty and, as readily seen from the third column of Fig. 10, leads to a vanishing result in the infinite-temperature limit $\beta\to 0$.

Note that the renormalized vertices that we have just introduced do not exhaust all possibilities. Indeed, the elementary vertices of Fig. 11, which involve two lines going in from the right, must be considered as nonrenormalizable vertices and will, of course, appear as such in our diagrammatic expression.

With the temperature-dependent renormalization of the vertices, we have thus eliminated all equilibrium correlations from the diagrammatic expansion for the af. The initial condition then merely reduces to the nonequilibrium initial state where spin b may eventually be involved in one correlation. More precisely, the most general structure of a diagram is given either by Fig. 12(a) or by Fig. 12(b), where the box represents the sum of all possible diagrams starting and ending with one semiconnection line.

These two structures are easy to combine; if we denote by $\Psi(M_a,M_b)$ the contribution of the box, where

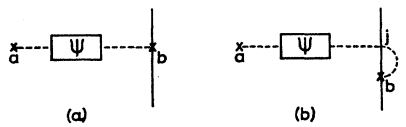

FIG. 12. Elimination of the nonequilibrium initial state.

[11] The existence of such a time t_1, for any equilibrium correlation is a consequence of Ref. 9.

[12] Except for case (2), we have given the contributions for one given direction of the arrows. Changing the direction of the arrows only modifies the sign of the analytical term.

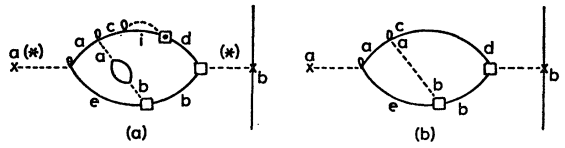

FIG. 13. Example of a skeleton: (a) graph; (b) skeleton.

the trace has been taken over all dummy spins, the sum of these two terms can be written as (see Rules A)

$$\Gamma_{ab}^{zz}(t)=\sum_j\sum_{M_j}\Psi(M_a,M_j)[\delta_{j,b}{}^{\mathrm{Kr}}M_j+(1-\delta_{j,b}{}^{\mathrm{Kr}})\times 2\beta\Phi_{jb}M_j]\sum_{M_b=\pm 1/2}M_b{}^2(\tfrac{1}{2})^3|_{M_a=1/2}$$

$$=\sum_j\sum_{M_j}\Psi(M_a,M_j)M_j(\tfrac{1}{2})^2\times[\delta_{j,b}{}^{\mathrm{Kr}}+(1-\delta_{j,b}{}^{\mathrm{Kr}})\tfrac{1}{2}\beta\Phi_{jb}]|_{M_a=1/2}. \quad (6.7)$$

Comparing with (3.9), we get

$$\Gamma_{ab}^{zz}(t)=4\sum_j\{\sum_{M_j}\Psi(M_a,M_j)M_j(\tfrac{1}{2})^2|_{M_a=1/2}\}\Gamma_{jb}^{zz}(0). \quad (6.8)$$

From the definitions (2.15) and (2.18), we then discover that the normalized af $\tilde{\Gamma}_{ab}(t)$, which is of main interest, is given, up to a factor of 4, by the contributions of the graphs of the type given in Fig. 10(a) only.

All correlations have thus now been eliminated from our general expansion and this leads to a considerable simplification of the diagrammatic technique. Indeed, $\tilde{\Gamma}_{ab}(t)$ can be calculated (up to a factor of 4) from Rules A, except that the vertices are now the renormalized and nonrenormalizable vertices of Figs. 10 and 11 and that all equilibrium correlations can be omitted.

VII. PROPAGATOR RENORMALIZATION

In RDL I, we discussed one method for getting rid of the unphysical t^2 factor in expressions of the type (6.1). It was recognized that this factor can be interpreted as resulting from the arbitrary long duration of the collision between two neighboring spins. Under these circumstances, it is not physically satisfactory to consider only two isolated spins and the interaction with the "bath" made of the remaining spins has to be taken into account explicitly. Because of this interaction, the information put on two given spins a and b at time t_1 diffuses away and, at time t_2, the remaining information on each of these spins is only $\Gamma(t_1-t_2)$.

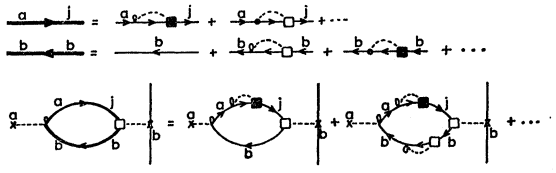

FIG. 14. An example illustrating Theorem IV.

Indeed, it was shown that an infinite resummation of graphs leads to the following modification:

$$\frac{t^2}{2!}=\int_0^t dt_1\int_0^{t_1}dt_2\to\int_0^t dt_1\int_0^{t_1}dt_2\Gamma^2(t_1-t_2)\sim t \quad (t\to\infty). \quad (7.1)$$

Once a t-growing transition probability can be defined, it is easy to derive kinetic equations according to well-known techniques (see Ref. 5). In the infinite temperature limit, this led to the results (1.2) and (1.3). This remormalization procedure was shown to be exact in the Weiss limit, although the kernel $\tilde{G}_q(t|\Gamma)$ was defined through an infinite series of graphs. However, its interest originated in the possibility of finding simple and soluble approximations for this kernel.

We shall use a similar method here. However, we shall generalize it in such a way that it leads to results where simple and soluble approximations can be found even near the critical point. In the infinite-temperature case, the renormalization was done with the direct af $\Gamma(t)$, our motivation being that, in that limit, the diffusion mechanism is fairly fast while the exchange interaction $J(i-j)$ is of short range; we then expect little interaction between the fractions $[1-\Gamma(t)]$ of the information on spins a and b, which spread over the bath. These effects were then classified in "higher-order" terms in the series expansion for the kernel $\tilde{G}_q(t|\Gamma)$.

Near the critical point, two new physical effects throw suspicion on this argument: (1) Diffusion processes are known to be slow near T_C, although one of the difficulties in the classical theories is precisely that they predict too slow a diffusion. (2) The effective interaction, described in the present theory by the renormalized vertices, has a very long range (the Fourier transform ϕ_q diverges at T_C when $q\to 0$). We thus expect that the interaction between the parts of the information which have diffused from spins a and b may become important near T_C. We shall now show how a different resummation procedure can be developed, leading to expressions where this effect is clearly apparent and where sensible approximations appear very naturally.

To this aim, we define the *skeleton* of a given graph as the diagram which is obtained by cutting off the self-energy insertions on all the plain and dotted lines which are not isolated. Here, a self-energy insertion is defined as a part of graph which starts with one plain (dotted) line and ends with one plain (dotted) line, the two lines carrying spin indices which can be either identical or different[13]; we also define an isolated line by the fact that cutting it makes the diagram fall in two pieces.

[13] These definitions are more general than in RDL I and II. Moreover, we use the nomenclature familiar from many-body theory although the analogy is purely topological and has no physical significance.

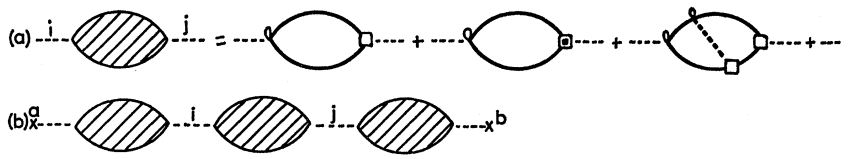

FIG. 15. Irreducible renormalized skeleton parts: (a) example; (b) general structure of $\tilde{\Gamma}_{ab}(t)$.

An example is given in Fig. 13, where the asterisks denote the two isolated lines; note that, in contrast with the definition given in RDL I and II, the skeleton of a graph is generally *not* itself a graph appearing in the expansion of $\tilde{\Gamma}_{ab}(t)$, because some lines carry two different spin indices. However, except for these indices, each skeleton is topologically identical to a graph contributing to $\Gamma_{ab}{}^{zz}(t)$.

We then have:

Theorem IV (of propagator renormalization): In the Weiss limit, the whole series of graphs for $\tilde{\Gamma}_{ab}(t)$ may be obtained by taking the sum of all skeleton graphs, i.e., skeletons where all nonisolated plain and dotted lines are replaced by corresponding heavy lines representing the sum of all self-energy insertions. The corresponding analytical contribution is obtained as for ordinary graphs (including vertex renormalization) except that (a) to each plain line, starting at time t_1 with spin i and ending at time t_2 with spin j, we now associate a factor

$$2\delta_{M_i,0}{}^{\mathrm{Kr}}\eta^{+1i}\delta_{M_j,0}{}^{\mathrm{Kr}}\tilde{\Gamma}_{ij}(t_1-t_2) \quad (i\neq j), \tag{7.2a}$$

$$\tilde{\Gamma}_{ii}(t_1-t_2)\delta_{M_i,0}{}^{\mathrm{Kr}} \quad (i=j); \tag{7.2b}$$

(b) to each heavy dotted line, we associate a factor

$$4M_i\tilde{\Gamma}_{ij}(t_1-t_2)M_j. \tag{7.3}$$

The first part of this theorem is of purely topological character and is established precisely as in RDL I (Theorem III); it is illustrated in Fig. 14.

The second part is more difficult to prove because, according to Rules A, self-energy insertions are still operators which, when inserted in a skeleton, act on whatever stands on their right. Note that this fact is explicit in (7.2a). However, the calculation parallels closely that given in RDL I for $\beta=0$ and will not be reproduced here. For the sake of illustration, one case is treated in detail in Appendix C.[14]

VIII. DERIVATION OF THE KINETIC EQUATIONS

In Secs. V–VII, we have derived a series of formal theorems, valid in the Weiss limit, which considerably simplify the series expansion for the normalized af $\tilde{\Gamma}_{ab}(t)$. Theorems I and II tell us that the dominant graphs can be built using only the basic components of Fig. 6. Theorem III and Eq. (6.8) allow us to eliminate all initial correlations, by the introduction of renormalized (temperature-dependent) vertices. Theorem IV further reduces the number of relevant graphs: Only skeletons should be considered, with, however, the renormalized (time-dependent) propagators of Eqs. (7.2) and (7.3).

At this stage, it is worthwhile to formulate the rules which give the exact formal expression for $\tilde{\Gamma}_{ab}(t)$ in terms of renormalized quantities.

Rules B: [(1)] Draw all possible renormalized skeletons (see Sec. VII) starting with a crossed dotted line b at time 0 and ending with a crossed dotted line a at time t. These graphs are constructed with the renormalized vertices of Fig. 10 (column b) and from the nonrenormalizable vertices of Fig. 11. The plain lines and the nonisolated dotted lines can carry one or two spin indices.

(2) Associate a factor $2\delta_{M_i,0}{}^{\mathrm{Kr}}\eta^{+1i}\delta_{M_j,0}{}^{\mathrm{Kr}}\tilde{\Gamma}_{ij}(t_1-t_2)$ $(i\neq j)$ or $\delta_{M_i,0}{}^{\mathrm{Kr}}\tilde{\Gamma}_{ii}(t_1-t_2)$ $(i\neq j)$ to a heavy plain line starting with spin j at time t_2 and ending with spin i at time t_1. Similarly the contribution of a heavy dotted line is $4M_iM_j\tilde{\Gamma}_{ij}(t_1-t_2)$.

(3) To each vertex, associate the contribution indicated in Figs. 10 and 11. Associate a factor M_b to the cross b at $t=0$. Operators and M-dependent factors are ordered as they appear in the graph.

[(4)] Multiply by a factor $4(\frac{1}{2})^m(-\lambda^2)^n\int d\tau^{2n}$ for a skeleton of order $2n$ involving m distinct spins (including a and b).

(5) Take the trace $(\sum_{M_i=\pm 1/2}\cdots)$ over all spins $i\neq a$ and set $M_a=\frac{1}{2}$ once all operations are performed.

(6) Sum over all dummy spin indices.

The great similarity with the Rules of RDL I for the infinite temperature case should be recognized. All the features brought in by the finite temperature are contained in the more complicated analytical contribution associated with vertices and lines. Yet, in the derivation of formal kinetic equations, the major role is played by the topological structure of the graphs and not by the explicit analytic expressions. We are thus able to use, without any deep modification, the scheme developed in RDL I; this will allow us to be very brief.

We first define an *irreducible renormalized skeleton part ij* as a renormalized skeleton starting at t_1 with an isolated dotted line j and ending at t_2 with an isolated dotted line i, with no intermediate state involving one isolated line. We denote the contribution associated with one irreducible skeleton part ij (numbered n) by

$$\tilde{G}_{ij}{}^{(n)}(t_1-t_2; M_i,M_j,\{M_{a_{ij}}\}\,|\,\tilde{\Gamma}_{st}), \tag{8.1}$$

[14] The reader who wants to prove Eq. (7.2) should first generalize Rules A to the transverse component $\Gamma_{ab}{}^{\perp}(t)$ (see Ref. 8).

where the functional dependence on $\tilde{\Gamma}_{st}$ has been exhibited, and α_{ij} denotes the spins, different from i and j, which appear in $\tilde{G}_{ij}^{(n)}$. This quantity is an operator, acting on whatever stands on its right; moreover, no trace is taken over the quantum numbers M_i, M_j, $M_{\alpha_{ij}}$. It thus cannot be directly calculated from Rules B, although it is readily obtainable therefrom as was shown in an analogous case in RDL I. We shall not need the explicit form of (8.1) here.

The sum of all such irreducible skeleton parts ij is schematically denoted by the "bubble" of Fig. 15(a) and the corresponding contribution is written as

$$\tilde{G}_{ij}(t_1-t_2; M_i,M_j,\{M_{\alpha_{ij}}\}\,|\,\tilde{\Gamma}_{st}) = \sum_n \tilde{G}_{ij}^{(n)}(t_1-t_2; M_i,M_j,\{M_{\alpha_{ij}}\}\,|\,\tilde{\Gamma}_{st}). \quad (8.2)$$

With these definitions, it is readily seen that the most general renormalized skeleton contributing to $\tilde{\Gamma}_{ab}(t)$ has the structure indicated in Fig. 15(b).

The analytical expression for $\tilde{\Gamma}_{ab}(t)$ is then easily seen to have the following form:

$$\tilde{\Gamma}_{ab}(t)=4\sum_{m=0}^{\infty}\sum_{i,s,l\cdots}\sum_{\{\alpha_{ai}\}\{\alpha_{is}\}\cdots\{M_{i\neq a}\}}\int_0^t dt_1\int_0^{t_1}dt_2\cdots\int_0^{t_{2m-1}} dt_{2m}\tilde{G}_{ai}(t_1-t_2; M_a=\tfrac{1}{2}, M_j, \{M_{\alpha_{ij}}\}\,|\,\tilde{\Gamma}_{kl}) \times\tilde{G}_{is}(t_3-t_4; M_j,M_s,\{M_{\alpha_{js}}\}\,|\,\tilde{\Gamma}_{uv})\cdots\tilde{G}_{lb}(t_{2m-1}-t_{2m}; M_l,M_b,\{M_{\alpha_{lb}}\}\,|\,\tilde{\Gamma}_{xy})M_b(\tfrac{1}{2})^N, \quad (8.3)$$

where, for convenience, we have summed over all $M_{i\neq a}$ and introduced a factor $(\frac{1}{2})^N$, in such a way that, for any spin β which does not appear explicitly in (8.3), we have $\sum_{M_\beta}\frac{1}{2}=1$. Note also that no exclusion is imposed on the spin indices i, s, $\cdots$, l, because this would introduce corrections of order Z^{-1} and would be negligible in the Weiss limit.

The analogy between Eqs. (8.3) and RDL I (5.3) is complete. The method followed in this latter paper to reduce the formal solution for $\tilde{\Gamma}_{ab}(t)$ to a kinetic equation can be followed step by step. We shall thus not reproduce this calculation and merely give the formal result. The following equation is obtained[15]:

$$\partial_t\tilde{\Gamma}_{ab}(t)=\sum_j\int_0^t dt' G_{aj}(t-t'\,|\,\tilde{\Gamma}_{st})\tilde{\Gamma}_{jb}(t'), \quad (8.4)$$

where the kernel $G_{aj}(t-t'\,|\,\tilde{\Gamma}_{st})$ is a function and not an operator, defined by

$$G_{aj}(t-t'\,|\,\tilde{\Gamma}_{st})=\sum_{(n)}G_{aj}^{(n)}(t-t'\,|\,\tilde{\Gamma}_{st}), \quad (8.5)$$

with

$$G_{aj}^{(n)}(t\,|\,\tilde{\Gamma}_{st})=4\sum_{\{\alpha_{aj}\}}\sum_{\{M_{\alpha_{aj}}\}}\sum_{M_j}\tilde{G}_{aj}^{(n)}(t; M_a=\tfrac{1}{2}, M_j, \{M_{\alpha_{aj}}\}\,|\,\tilde{\Gamma}_{st})M_j(\tfrac{1}{2})^{m+2}; \quad (8.6)$$

here m denotes the number of spins in the set α_{aj}.

Because the kernel $G_{aj}(t\,|\,\tilde{\Gamma}_{st})$ plays a central role in applications of the theory, it is very helpful to have prescriptions which allow to calculate it directly, without using the auxiliary operator $\tilde{G}_{aj}^{(n)}$. These rules are immediate to obtain once the formal similarity between Eqs. (8.5) and (8.6) and Eq. (6.8) is noted. The only difference lies in the fact that G_{ab} corresponds to *irreducible* renormalized skeleton parts while $\tilde{\Gamma}_{ab}(t)$ is given by the sum of all renormalized skeletons. As a consequence, the rules for constructing $G_{ab}(t_1-t_2\,|\,\tilde{\Gamma}_{st})$ will be again Rules B except that the bracketed points [(1)] and [(4)] should be modified as follows.

Rules C: (1) Draw all possible *irreducible* renormalized skeletons $\cdots$

(4) Multiply by a factor $4(\frac{1}{2})^m(-\lambda^2)^n\int_{t_1}^{t_2}d\tau^{2n-1}$ for a graph of order n involving m distinct spins (including a and b).

It is often convenient to work with the Fourier transform of $\tilde{\Gamma}_{ab}(t)$,

$$\tilde{\Gamma}_q(t)=\sum_a\tilde{\Gamma}_{ab}(t)\exp[iq(a-b)]. \quad (8.7)$$

If we define

$$\tilde{G}_q(t\,|\,\tilde{\Gamma}_{q'})=\sum_b G_{ab}(t\,|\,\tilde{\Gamma}_{st})\exp[iq(a-b)], \quad (8.8)$$

Eq. (8.4) transforms at once into

$$\partial_t\tilde{\Gamma}_q(t)=\int_0^t\tilde{G}_q(t-t'\,|\,\tilde{\Gamma}_{q'})\tilde{\Gamma}_q(t')dt', \quad (8.9)$$

which is the final form of our kinetic equation for the af in the Heisenberg spin system at finite temperature.

Let us stress once more that this result is exact in the Weiss limit only; although we hope that this equation will still approximately describe the behavior of a realistic system, where Z is finite, we do not know whether an equation of the same structure[16] can be derived exactly in the latter case. Precisely as in the

[15] Although G_{aa} is larger by a factor Z than any other $G_{ab}(a\neq b)$, we have not found it convenient here to separate this term, as was done in RDL I.

[16] Of course, using a projection operator technique [see, for instance, R. Zwanzig, Phys. Rev. 124, 983 (1961)], it is trivial to derive a kinetic equation of the type $\partial_t\tilde{\Gamma}_q(t)=\int_0^t\tilde{G}_q(t-t')\tilde{\Gamma}_q(t')dt'$ independent of the value of Z. However, the important feature of the kernal of Eq. (8.9) is its *explicit dependence on* $\tilde{\Gamma}_{q'}$, which has only been established in the Weiss limit.

infinite temperature case, we expect, of course, that

$$\tilde{\Gamma}_q(t) \to 0, \quad t \to \infty, \tag{8.10}$$

although, for small enough q, the characteristic time of this decay can become very large. This in turn should imply a property analogous to (1.4).

The reorganization of the perturbation series for $\tilde{\Gamma}_{ab}(t)$ with the help of renormalized vertices and propagators leads thus, hopefully, to a kinetic equation in which all quantities are well behaved in the limit of long times. This is the basis for an explicit though approximate calculation of $\tilde{\Gamma}_q(t)$, as will be discussed in the next paper of this series.

APPENDIX A. MATRIX ELEMENTS OF THE LIOUVILLE-VON NEUMANN OPERATOR

For the sake of reference, we list here the matrix elements of the Liouville-von Neumann operator, as derived in RDL I Eqs. (II.19). The only nonvanishing transverse matrix elements are the following [see Fig. 1(a) (1)-(4)]:

$$\mu_i=0,\ \mu_j=0: \quad \langle 0_i,0_j,\{\mu\}'|\mathcal{K}_{ij}{}^{+-}|-1_i,+1_j,\{\mu\}'\rangle = -J(i-j)\eta_{ij}\delta_{M_i,0}{}^{\mathrm{Kr}}\delta_{M_j,0}{}^{\mathrm{Kr}}, \tag{A1}$$

$$\mu_i=1,\ \mu_j=-1: \quad \langle 1_i,-1_j,\{\mu\}'|\mathcal{K}_{ij}{}^{+-}|0_i,0_j,\{\mu\}'\rangle = -J(i-j)\delta_{M_i,0}{}^{\mathrm{Kr}}\delta_{M_j,0}{}^{\mathrm{Kr}}\eta_{ij}, \tag{A2}$$

$$\mu_i=1,\ \mu_j=0: \quad \langle 1_i,0_j,\{\mu\}'|\mathcal{K}_{ij}{}^{+-}|0_i,1_j,\{\mu\}'\rangle = -J(i-j)\delta_{M_i,0}{}^{\mathrm{Kr}}\eta_{ij}\delta_{M_j,0}{}^{\mathrm{Kr}}, \tag{A3}$$

$$\mu_i=0,\ \mu_j=-1: \quad \langle 0_i,-1_j,\{\mu\}'|\mathcal{K}_{ij}{}^{+-}|-1_i,0_j,\{\mu\}'\rangle = -J(i-j)\delta_{M_j,0}{}^{\mathrm{Kr}}\eta_{ij}\delta_{M_i,0}{}^{\mathrm{Kr}}, \tag{A4}$$

where η_{ij} is the displacement operator defined by (4.3) and $J(i-j)$ denotes the exchange interaction between spins i and j. The longitudinal matrix elements obey [see Fig. 1(b)]

$$\langle\mu|\mathcal{K}_{ij}{}^{zz}(M)|\mu\rangle = -J(i-j)[M_i\mu_j+M_j\mu_i]. \tag{A5}$$

It should be noted that the Kronecker functions in (A1) and (A4) appear on the side where the corresponding μ index is not vanishing. This property is important for justifying Rules A, where these Kronecker functions are associated with the plain lines and not with the vertices.

APPENDIX B. PROOF OF THEOREM II

In analogy with RDL I, we introduce the topological index Z_i of a vertex i; it is equal to the number of spins over which we may sum freely, at this vertex, if we read a graph from right to left. There are seven types of elementary vertices, denoted by i ($i=1, 2, \cdots 7$), which are indicated on Fig. 16(a). Similarly, we define the topological index for each equilibrium pair correlation: $Z_8=Z^{-1}$ for the transverse correlations and $Z_9=Z^{-1}$ for the longitudinal ones; these values follow from the estimate (5.2) [see Fig. 16(b)]. Similarly, we take

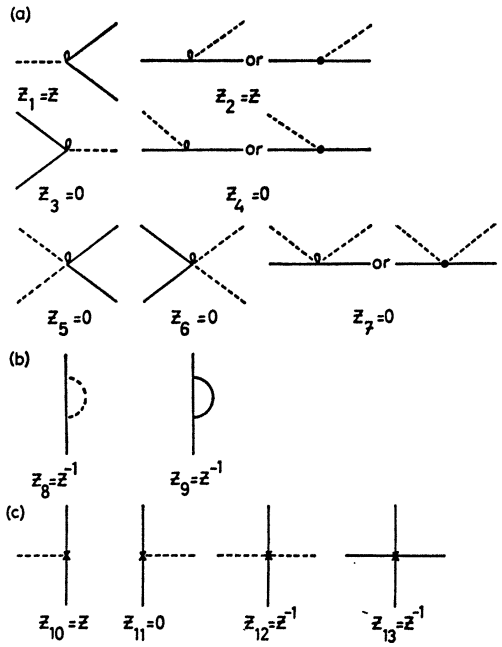

FIG. 16. Topological indices: (a) elementary vertices; (b) equilibrium correlations; (c) nonequilibrium initial states.

into account that the cross describes the *given* spin b; this imposes further restrictions expressed by the topological indices $Z_{10}=Z^{-1}$, $Z_{11}=0$, $Z_{12}=Z^{-1}$, $Z_{13}=Z^{-1}$, according to the possible initial states, as indicated in Fig. 16(c).

Consider an arbitrary graph with $a\neq b$, made of m_i ($m_i\geq 0$) elements of type i ($i=1, \cdots 13$), with the restriction

$$\sum_{i=10}^{13} m_i = 1, \tag{B1}$$

because there is only one cross per graph.

From the definition of the topological index, the order in Z of the graph, denoted by O_Z, is immediately found to be

$$O_Z = m_1+m_2-m_8-m_9-m_{10}-m_{12}-m_{13}, \tag{B2}$$

while the order in λ, denoted by O_λ, is simply

$$O_\lambda = \sum_{i=1}^{7} m_i. \tag{B3}$$

We remark that each plain line which is created has to disappear; this implies that

$$2(m_1+m_5) = 2(m_3+m_6+m_8). \tag{B4}$$

A similar condition for the dotted lines leads to

$$1+m_2+m_3+2m_6+m_{11} = m_1+m_4+2m_5+2m_9+m_{10}. \tag{B5}$$

Combining (B2, B3, B4, and B5), we get

$$O_Z = \tfrac{1}{2}O_\lambda - \tfrac{3}{2} - \tfrac{1}{2}(m_5+m_6+m_7) + \tfrac{1}{2}(m_{10}+m_{11}). \tag{B6}$$

Two cases are to be discussed separately:

(A) O_λ *is even:* The order O_Z obviously has to be an integer; the largest possible order is thus obtained by choosing

$$m_{10} \quad \text{or} \quad m_{11}=1, \tag{B7}$$

$$m_5=m_6=m_7=0. \tag{B8}$$

We then get

$$O_Z{}^{\max}=\tfrac{1}{2}O_\lambda-1, \tag{B9}$$

and we also see that, among all *a priori* possible structures, the graphs of largest order are constructed with the basic components of Figs. 6(a)–6(c) only.

(B) O_λ *is odd:* The largest integer order O_Z is here obtained by choosing

$$m_5=m_6=m_7=0 \tag{B10}$$

and

$$m_{10}=m_{11}=0. \tag{B11}$$

This leads to

$$O_Z{}^{\max}=\tfrac{1}{2}O_\lambda-\tfrac{3}{2},$$

while, comparing (B1) and (B11), we see that

$$m_{12} \quad \text{or} \quad m_{13}=1. \tag{B12}$$

It is easily verified by combining graphs differing only by the direction of the arrows that the structure 13 of Fig. 16 always gives zero for an odd-order graph. We thus conclude that, in case O_λ is odd, the graphs are constructed with the basic components of Figs. 6(a), 6(b), and 6(d).

The case $a=b$ is treated similarly; the time dependence of a graph and its real or imaginary character are trivial to obtain.

APPENDIX C. AN EXAMPLE OF PROPAGATOR RENORMALIZATION

We discuss here the effect of the self-energy insertion drawn in Fig. 17(b) and show that it amounts to weight the heavy dotted line of Fig. 17(a) by a factor $4M_iM_j\tilde{\Gamma}_{ij}(t_1-t_2)$. Note that in this figure, the vertices at times t_1 and t_2 have been specified. The general proof of Eq. (7.3) thus requires all possible vertices to be considered. This makes the complete calculation fairly long, and we limit ourselves here to the case of Fig. 17.

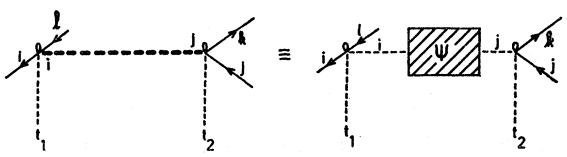

FIG. 17. An example of self-energy insertion.

Schematically, the contribution C of an arbitrary graph involving Fig. 17 as a part can be written as

$$C=\cdots\sum_{M_j}\cdots\delta_{M_i,0}{}^{\mathrm{Kr}}(-J_{il})\eta_{il}\Psi(M_i,M_j) \times(-J_{kj})\mu_{kj}\delta_{M_j,0}{}^{\mathrm{Kr}}\cdots. \tag{C1}$$

In this equation, the dots indicate both the time factors (which are trivial to handle) and the part of C which is not the particular insertion we discuss; $\Psi(M_i,M_j)$ is the most general self-energy insertion starting with spin j and ending with spin i; it depends, of course, on a set of dummy spin indices $\{\alpha_{ij}\}$, but all operations with these spins are formally considered as performed; $\Psi(M_i,M_j)$ is thus simply an operator depending on $\eta^{\pm 1_i}$, $\eta^{\pm 1_j}$, M_i, and M_j.

Because of the factor $\delta_{M_j,0}{}^{\mathrm{Kr}}$, this operator Ψ does not act on the dots on the right, although they depend on M_j [see RDL I, Eq. (A3)]; similarly, because of the factor $\delta_{M_i,0}{}^{\mathrm{Kr}}$, the dots on the left do not operate on $\Psi(M_i,M_j)$, although they depend on $\eta^{\pm 1_i}$.

From Eqs. (6.8) and (2.18), we see that

$$4\sum_{M_j}\Psi(M_i,M_j)M_j(\tfrac{1}{2})^2\big|_{M_i=1/2}=\tilde{\Gamma}_{ij}. \tag{C2}$$

Moreover, symmetry considerations allow us to deduce from (C2) that

$$\Psi(\tfrac{1}{2},\tfrac{1}{2})=-\Psi(\tfrac{1}{2},-\tfrac{1}{2})=-\Psi(-\tfrac{1}{2},\tfrac{1}{2}) =\Psi(-\tfrac{1}{2},-\tfrac{1}{2})=\tilde{\Gamma}_{ij} \tag{C3}$$

[see RDL I, Eq. (III.10) for a similar example].

Let us then perform explicitly the displacement operations in Eq. (C1); from the definitions (2.9) and (4.3), we get

$$\begin{aligned}C=\cdots\sum_{M_j}\cdots\delta_{M_i,0}{}^{\mathrm{Kr}}(-J_{il})(-J_{kj})[&\eta^{-1_i}\eta^{+1_l}\Psi(-\tfrac{1}{2},-\tfrac{1}{2})\\ &\times\eta^{-1_k}\eta^{+1_j}-\eta^{+1_i}\eta^{-1_l}\psi(\tfrac{1}{2},-\tfrac{1}{2})\eta^{-1_k}\eta^{+1_j}-\eta^{-1_i}\eta^{+1_l}\\ &\times\Psi(-\tfrac{1}{2},\tfrac{1}{2})\eta^{+1_k}\eta^{-1_j}+\eta^{+1_i}\eta^{-1_l}\Psi(\tfrac{1}{2},\tfrac{1}{2})\eta^{+1_k}\eta^{-1_j}]\\ &\times\delta_{M_j,0}{}^{\mathrm{Kr}}\cdots.\end{aligned} \tag{C4}$$

Using (C3), this result is easily seen to be identical to

$$C=\cdots\sum_{M_j}\cdots\delta_{M_j,0}{}^{\mathrm{Kr}}(-J_{il})\eta_{il} \times4M_iM_j\tilde{\Gamma}_{ij}(-J_{kj})\eta_{kj}\delta_{M_j,0}{}^{\mathrm{Kr}}, \tag{C5}$$

as may be checked by direct evaluation. Comparison between (C1) and (C5) then establishes the required result.